Feed Forward Initialization of Hysteretic Systems

camera ready version submitted at 30 Aug 2010 to 49th IEEE Conference on Decision and Control, December 15-17, 2010 Atlanta, Georgia USA.

P.J. van Bree, C.M.M. van Lierop, P.P.J. van den Bosch

Abstract— **The paper analyzes a strategy to force step-convergent dynamical hysteretic systems to a well-defined output value using only feed forward. Due to the multi-valued input-output relation of hysteresis, the relation between a constant input and the corresponding steady-state output is not unique. By using a well-designed input trajectory, based on qualitative system behavior only, such a system can still be forced to a predefined output value. Moreover, for reasons of performance the initialization time has to be as short as possible. The rate-independent Duhem and the multi-play hysteresis models are used to illustrate, analyze and synthesize an appropriate initializing input to obtain the required output without any sensor information. Dynamics are included using the nonlinear feedback model with dead-zone.**

I. INTRODUCTION

Feed forward control of dynamical hysteretic systems with transient inputs is complicated since sufficiently accurate predictive models are still lacking. However, with the help of feed forward initializing input trajectories such systems can still be forced to a unique output value. The design of such trajectories is based on the qualitative behavior of hysteresis, not on inverse modeling. Consequently, this allows for a well-defined reset of the system. In automated processes such a reset should take as less time as possible.

The physical systems considered are dynamical hysteretic step-convergent systems as explained in section II. Examples are piezoelectric and ferromagnetic systems. Feedback control of such systems is an option if the sensor information is accurate enough. Hysteresis is then still a performance limiting factor [1], [2], [3]. However, in a system where the accuracy, bandwidth and/or noise properties of the sensor are the bottlenecks, a feed forward approach is required.

An example is found in electron microscopy where considerable hysteresis is present owing to the massive ferromagnetic yoke of the electromagnetic lenses [4]. Images are recorded with a constant magnetic field. The reference profile is non-periodic. Any deviation of this field larger than 0.01% of the total magnetic field range results in an unacceptable image quality. Magnetic field sensors are currently not available in these machines. The search for such a sensor is complicated by the challenging requirements: a resolution of μT versus an amplitude range of about a Tesla. And a time range that varies from $10ms$ transition-time between setpoints versus drift requirements over hours. Next to that the sensor has to fit into the 3d lens geometry without disturbing the electron optic behavior. Feedback control based on microscopy-images is limited by the image processing-rate and the limited range in which the image contains enough information for control. Consequently, feedback strategies are not trivial.

However, the input of the magnetic lens system (current) can be measured and controlled very accurately. Since images in electron microscopy are recorded in steady state, the reproducibility of fixed points in steady state using only feed forward is under study. Reproducibility of the lens settings, is essential for automated microscopy procedures to work fast, accurate and without intervention of the operator.

In [4] an experimental start is made by testing with feed forward initialization trajectories on a magnetic lens system of a commercially available electron microscope. With the use of these trajectories, the state of the lens system is forced to a pre-defined value such that experiments are made reproducible. Although the presented trajectories are sufficiently accurate, its duration is rather long (up to 20s). For scientific experiments this needs not be a problem. However, for automated procedures in the industry less time is beneficial.

With the use of models that are both hysteretic and dynamic, the relevant parameters for optimization of initialization trajectories are obtained. Section II starts with the required definitions. In the case of quasi-static inputs the hysteresis effect can be considered independent from dynamics. The Duhem and multi-play model are taken as examples to provide the initialization requirements for this situation in section III. The approach for the dynamical situation is introduced by the nonlinear feedback model with dead-zone [5] in section IV-A.

II. DEFINITIONS

A. Convergence

Given a (non-)linear stable, time invariant, and controllable dynamical system:

$$\begin{aligned} \dot{x}(t) =& F(x(t), u(t), x_0), \quad x_0 = x(t_0) \\ y(t) =& G(x(t), u(t)) \end{aligned} \tag{1}$$

Where $u(t) \in \mathbb{R}^m, x(t) \in \mathbb{R}^n, y(t) \in \mathbb{R}^l$ represent the input, the state and the output. The system (1) fulfills the *step convergence* property [6], which implies that the state

This work is carried out as part of the Condor project, a project under the supervision of the Embedded Systems Institute (ESI) and with FEI company as the industrial partner. This project is partially supported by the Dutch Ministry of Economic Affairs under the BSIK program.

P.J. van Bree, C.M.M. van Lierop and P.P.J. van den Bosch are with the Department of Electrical Engineering, Eindhoven University of Technology. p.j.v.bree@tue.nl

converges to a constant $\bar{x}$ for all combinations $(\bar{u}, x_0)$.

$$\begin{aligned}\bar{x} =& \arg_x \{F(x, \bar{u}, x_0) = 0\} \\ \bar{y} =& G(\bar{x}, \bar{u})\end{aligned} \tag{2}$$

If the difference between two trajectories starting from two different initial conditions $x_0, x_0 + \delta$ vanishes for all perturbations $\delta \in \mathbb{R}^n$, the system has the *fading memory* property, [7, p.74]:

$$\lim_{t\to\infty} \{F(x(t), u(t), x_0) - F(x(t), u(t), x_0 + \delta)\} = 0 \tag{3}$$

Condition (3) implies, that the steady state value $\bar{y}$ only depends on the applied constant input $\bar{u}$ and not on the initial condition. In case of feed forward setpoint regulation of a system that satisfies (3), any fixed point $\bar{y}(\bar{u})$ can be *reproduced* by applying the constant input $\bar{u}$ at any time t_0 for any initial condition x_0.

The time it takes for the output of the system to converge to within a distance ϵ_1 of the limit value $\bar{y}$ from a specific $x(t_0)$ and $\bar{u}$ is defined as convergence time t_c:

$$\begin{aligned}t_c = \min_t \{t - t_0\}, \\ \text{s.t. } |y(\tau) - \bar{y}| \le \epsilon_1, \quad \forall \tau \ge t \ge t_0\end{aligned} \tag{4}$$

If both the initial conditions and the input are in a bounded set, $x_0 \in \mathcal{X}, \quad \bar{u} \in [u_{min}, u_{max}] = \mathcal{U}$ an upper bound on the convergence time is defined as:

$$\hat{t}_c = \max_{x_0\in\mathcal{X},\bar{u}\in\mathcal{U}} t_c(\bar{u}, x_0) \tag{5}$$

B. Systems with Hysteresis

The notion of step-convergence (2) is introduced in [6] for dynamical systems with hysteresis. The fading memory property (3) does, however, not hold for hysteretic systems. The steady state output value $\bar{y}$ is then a function of both the constant input $\bar{u}$ and the initial condition x_0. Consequently, a fixed point $\bar{y}(\bar{u})$ can not be reproduced by applying $\bar{u}$ for $\hat{t}_c$ seconds. To study the possibility of reproducing a fixed point, the convergence of nonlinear dynamical systems with hysteresis is studied for a wider class of inputs.

C. Periodic Trajectories

Consider a class of periodic inputs u_T defined as:

$$u_T(t) = u_T(t+kT) = a_0 + a_1\Phi(2\pi t/T + \theta), \quad k \in \mathbb{N} \tag{6}$$

u_T is defined by function Φ, $||\Phi||_\infty = 1$, period T, phase θ, offset a_0 and peak to peak amplitude $2a_1$. The response to u_T is periodic if

$$\lim_{t\to\infty} (y(t+m\Gamma, u_T, x_0) - y(t, u_T, x_0)) = 0, \quad \forall m \in \mathbb{N} \tag{7}$$

When the smallest possible Γ for which (7) holds equals T, the period of the output is equal to the period of the source, $y_\Gamma = y_T$.

If (7) holds for all u_T, x_0, the state of system (1) converges to a periodic trajectory, independent of x_0 and independent of the parameters of u_T. The trajectory $(u_T(t), y_T(t))$ is then a closed orbit and is further referred to as $\phi(u_T(t), x_0)$. This orbit is considered as a continuous periodic set of points irrespective of its phase. Therefore, two orbits $\phi_1(u_T(t_1), x_0), \phi_2(u_T(t_2), x_0)$ are considered being equal if there exists a time shift $0 \le |\tau| \le T$ such that the set of points described by both is the same and is evaluated in the same order:

$$\{y_T(t_1, u_T(t_1), x_0) - y_T(t_2 + \tau, u_T(t_2 + \tau), x_0)\} = 0 \tag{8}$$

If the system converges to the same orbit for all perturbations $\delta \in \mathbb{R}$ on x_0 then $\phi(u_T(t))$ is only determined by the input and is independent of x_0:

$$\phi(u_T(t), x_0) = \phi(u_T(t), x_0 + \delta), \quad \forall u_T(t), x_0, \delta \tag{9}$$

In [8] the terminology *(non-) local memory* is introduced which is widely used in literature about hysteresis. Although the formulation in this paper is different, any hysteretic system for which (9) holds is said to have local memory. Otherwise it has non-local memory.

If the orbit depends on the initial condition, it is still possible that for a limited set $\mathcal{X}$ and specific parameters of u_T a unique orbit is obtained. A periodic input trajectory that forces the system into a unique closed orbit $\phi(u_T), \quad \forall x_0 \in \mathcal{X}$ is called an *initialization trajectory*, u_{ini}.

III. QUASI-STATIC BEHAVIOR

An important subset of hysteresis models is the class of *rate-independent* models. A system is rate independent if the set of points connected by $(u(t), y(t))$ is the same for any time scaling on the input. Consider a continuous increasing function $\eta : [0, T] \to [0, T]$ satisfying $\eta(0) = 0$ and $\eta(T) = T$ is an admissible time transformation [2]. For a given piecewise-monotone input u the system E is rate-independent if:

$$x(\eta(t)) = E(u(t), x_0)(\eta(t)) = E(\eta(u(t)), x_0) \tag{10}$$

This property is often illustrated by the characteristic that the state only depends on the extremums in the input (the points where $\dot{u}$ changes sign, often called the amplitude trajectory), [8].

For dynamical systems with hysteresis, a rate-independent approximation can be made for *quasi-static* inputs. Variation of the signals is then so slow that the influence of the dynamics of the system can be neglected. Every point of the trajectory (u, y) can then be considered a fixed point $(\bar{u}, \bar{y})$.

Two examples of initialization trajectories for rate-independent hysteresis models will be given as an illustration.

A. Duhem Hysteresis Model

1) Model Description: As an example an implementation of a Duhem model is considered, [9],[10]:

$$\begin{aligned}\dot{x} =& h_1|\dot{u}|\,[h_2 u - x] + h_3\dot{u}, \quad x(t_0) = x_0 \\ =& \dot{u}\,(h_1 \text{sign}(\dot{u})\,[h_2 u - x] + h_3) \\ y =& x\end{aligned} \tag{11}$$

The three parameters are all constants $h_1 > 0, 0 < h_3 < h_2 < 2h_3$. Equation (11) can be rewritten such that it only depends on $\text{sign}(\dot{u})$ and not on $\dot{u}$ itself:

$$\frac{dx}{du} = h_1 \text{sign}(\dot{u}) \left[h_2 u - x\right] + h_3, \quad x(t_0) = x_0 \tag{12}$$

The set of possible initial conditions $x_0 \in \mathcal{X}$ is bounded by $x_{llim} = (h_2 u - \frac{h_2 - h_3}{h_1}) \leq x_0 \leq x_{ulim} = (h_2 u + \frac{h_2 - h_3}{h_1})$.

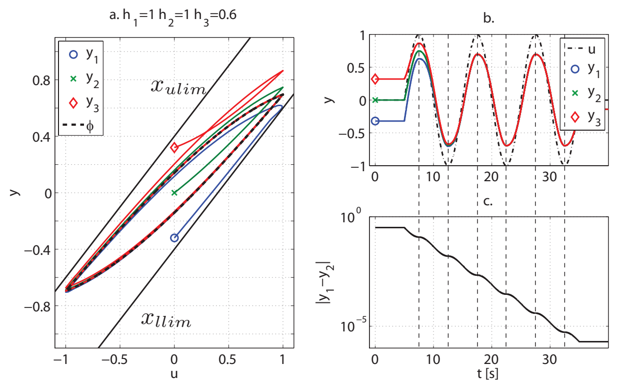

Fig. 1. Simulation of the Duhem model (12) for different initial conditions. a. The input-output plot (u, y). The dashed line shows the closed orbit $\phi(u_T)$. b. The response for $u_T = \sin(2\pi/T), T = 10s$ in the time-domain. c. The difference between trajectories $|y_1(t) - y_2(t)|$ on a logarithmic scale.

2) Available initialization trajectories: Differential equation (12) becomes linear for piecewise monotonically increasing or monotonically decreasing input segments, since $\text{sign}(\dot{u})$ is then equal to either ± 1. The analytic solution is formulated as follows:

$$y = h_2 u \tag{13a}$$

$$- \text{sign}(\dot{u}) \frac{h_2 - h_3}{h_1} \left(1 - \exp\left(-\text{sign}(\dot{u}) h_1 (u - u_0)\right)\right) \tag{13b}$$

$$+ (x_0 - h_2 u_0) \exp\left(-\text{sign}(\dot{u}) h_1 (u - u_0)\right) \tag{13c}$$

The main term of the response is a line (13a). The larger the amplitude of the increasing (or decreasing) segment $(u - u_0))$ (13b), the more y approaches the lower asymptote x_{llim}. The third component (13c), takes into account the initial condition which vanishes exponentially.

The difference between two trajectories starting from different initial conditions, $x_1(t_0) = x_{01}, x_2(t_0) = x_{02}$ subject to the same input u is:

$$|y_1 - y_2| = |x_{01} - x_{02}| \exp\left(-\text{sign}(\dot{u}) h_1 (u_{\uparrow} - u_0)\right) \tag{14}$$

The larger the magnitude $|u - u_0|$, the smaller the difference between y_1 and y_2 is. From analysis of the analytic expression for periodic inputs it can be derived (as is done in [10]) that the solution converges to a periodic orbit ϕ that is independent of x_0. The position of the resulting orbit is always around the line $y = h_1 u$. All possible u_T (6) can serve as initializing trajectories. This is a general property of models with local memory. From the notion of a quasi-static input and a rate-independent model structure, it makes no sense to express the rate of convergence in time. However, from the analysis it follows that the higher the amplitude a_1, the lower the number of periods that is required to initialize the model to a certain degree. The period time T has no influence on the resulting orbit, where the offset a_0 controls its position. The number and sequence of extremums in the function Φ influences the set of points described by the orbit. The phase θ is such that the trajectory starts at u_0.

3) Example: As an illustration, Fig. 1 shows the response to $u_T = sin(2\pi/T)$ plot for three different initial conditions. All three converge to $\phi(u_T)$. The difference $|y_1 - y_2|$ in time is shown on a logarithmic scale in subplot c. Note that at the points where $\dot{u}$ changes sign, convergence towards $\phi(u_T)$ is slower.

B. Multi-play Hysteresis Model

1) Model Description: Another common way of modeling rate-independent hysteresis is a multi-play approach consisting of a parallel connection of N weighted play (or backlash) operators $p(u, x_0, \Delta)$ where 2Δ is the width of the play (e.g. [11], [12]). This model is also called the Prandtl-Ishlinskii model of which an extended analysis is presented in [13], [14] [15] .

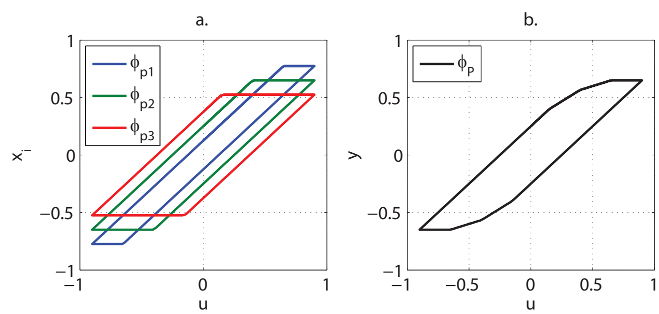

Fig. 2. Illustration of the multi-play hysteresis model(15) with $\Delta_1 = 0.25, \Delta_2 = 0.5, \Delta_3 = 0.75, \quad w_{1,2,3} = 1, \quad x_{01} = x_{02} = x_{03} = 0$, $u_T = 0.9 \sin(\pi t)$.

$$\begin{aligned} x_i &= p(u, x_{0i}, \Delta_i) = \max(\min(x_{0i}, u + \Delta_i), u - \Delta_i), \\ y &= P(u, x_0, \Delta) = \frac{1}{N} \sum_{i=1}^{N} w_i p(u, x_{0i}, \Delta_i), \\ &\Delta_i \geq 0, w_i \geq 0 \end{aligned} \tag{15}$$

2) Available Initialization Trajectories: In this section it will be shown that a multi-play model with an arbitrary set of Δ's can be initialized by a sequence that contains both the maximum and minimum input. Since this model contains a parallel connection there is no interaction among the different operators. To establish the parameter conditions of a periodic input (6), such that it is an initialization trajectory of the multi-play model, it is sufficient to study the properties for a single element.

The play operator is defined symmetric around the origin. The set $\mathcal{X}$ is bounded by $u - \Delta \leq x_0 \leq u + \Delta$ for $|u| \leq$

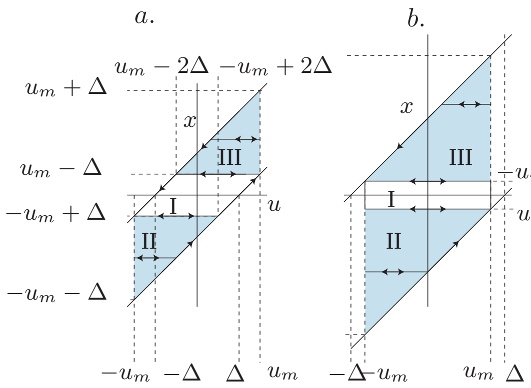

Fig. 3. Illustration of two play operators $a.u_m \geq \Delta$, $b.u_m < \Delta$

u_m. Fig. 3 represents $p(u, x_0, \Delta)$ for $u_m \geq \Delta$ ($a.$) and for $u_m < \Delta$ ($b.$).

In each case, three regions (I, II, III) are indicated. For both cases a and b it holds that if $(x_0, u_0) \in I$ then x stays in $I, \forall |u| \leq u_m$. Consider $p_1(u, x_{01} \in II, \Delta_1)$, and $p_2(u, x_{02} \in III, \Delta_2)$. For $\Delta < u_m$ it follows from (15) that $u_{ini} = [u_0, u_m, u_m - 2\Delta]$ or $u_{ini} = [u_0, -u_m, -u_m + 2\Delta]$ is the minimal sequence of points that initializes both p_1 and p_2. For the situation that $u_m \leq \Delta$ (case b) the initialization sequences becomes $u_{ini} = [u_0, u_m, -u_m]$ or $u_{ini} = [u_0, -u_m, u_m]$.

This result implies that only a trajectory containing both u_m and $-u_m$ initializes the multi-play model. However, a single period is sufficient. This condition is known as the 1^{st}-order wiping out property.

The resulting orbit ϕ is the sum of the orbits of the individual elements. If $\max u_T = u_m$, $\min u_T = -u_m$ and Φ has only 1 maximum and 1 minimum, then for case a ϕ_i is the boundary of region I. For case b ϕ is a line with offset x_0 if $x_0 \in I$, offset u_m if $x_0 \in III$ and offset $-u_m$ if $x_0 \in II$. The phase θ is again such that the trajectory starts at u_0.

IV. DYNAMICAL HYSTERETIC SYSTEMS

In this section the combination of dynamics and hysteresis is introduced, which results in so-called *rate-dependent models* of hysteresis.

A. Nonlinear Feedback Model with Dead-zone

The rate-independent play operator (15) is a nonlinear element with memory, which makes the analysis of (feedback) systems with such an element complicated. A possible way to avoid this, is to introduce similar behavior using building blocks of linear dynamical systems and (sector bounded) static nonlinearities. In [5] this class is called nonlinear feedback models of hysteresis. An example of a framework for analysis is found in [16].

1) Model Description: The general block scheme is shown in Fig. 4 a where Θ represents the static nonlinearity. A subset that approaches the behavior of play models for

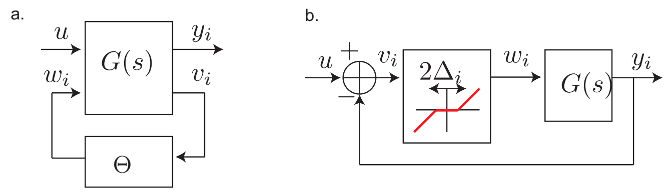

Fig. 4. Block diagram of a nonlinear feedback model. Left a. the general version with static nonlinearity Θ. Right b. The specific implementation with dead-zone analyzed in this paper.

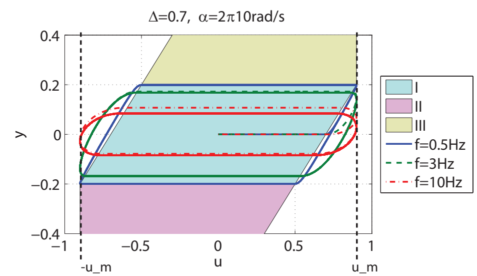

Fig. 5. Convergence of a single section of the nonlinear feedback model to an orbit ϕ. The initial condition is set to 0. In all three cases a sine-wave excitation is used.

quasi-static inputs [11] is the nonlinear feedback model where the nonlinearity Θ is a dead-zone:

$$w = d_{2\Delta}(v) = \max(\min(0, v + \Delta), v - \Delta) \tag{16}$$

Here, $2\Delta \geq 0$ is the width of the dead-zone. In a similar way as with the multi-play model, a parallel connection of multiple sections of nonlinear feedback models with a dead-zone can be defined, [11]:

$$\begin{aligned} \dot{x}_i(t) &= Ax_i(t) + Bd_{2\Delta_i}(u(t) - y_i(t)), \quad x_i(t_0) = x_{0i} \\ y_i(t) &= Cx_i \\ z(t) &= \frac{1}{N}\sum_{i=1}^{N} w_i y_i(t), \quad w_i \geq 0 \end{aligned} \tag{17}$$

$A \in \mathbb{R}^{n\times n}, B \in \mathbb{R}^{n\times 1}, C \in \mathbb{R}^{1\times n}$, with A, B, C minimal and given in the controllable canonical form. Each section can have its own Δ. $z(t)$ is the output of the weighted sections. A single section is shown in Fig. 4 b. The specific structure of a section approaches the behavior of a single play operator for quasi-static excitation. Therefore, Δ for the play operator and for the nonlinear feedback model are described by the same symbol. The memory of the play operator is now captured by the memory of the dynamical system $G(s)$. For the case $\Delta = 0$, the system (17) is a linear system denoted by $H(s) = (G + I)^{-1}G$.

For sake of clarity, one of the most simplified examples is taken. $G(s)$ represents a gain and an integrator, $G(s) = \frac{\alpha}{s}$ in (17) $A = 0, B = \alpha, C = 1$. The transfer function of the linear version $H(s) = \frac{\alpha}{s+\alpha}$ with $\Delta = 0$ is a first order low-pass filter of which the output in the time-domain is denoted with $y_H(t)$.

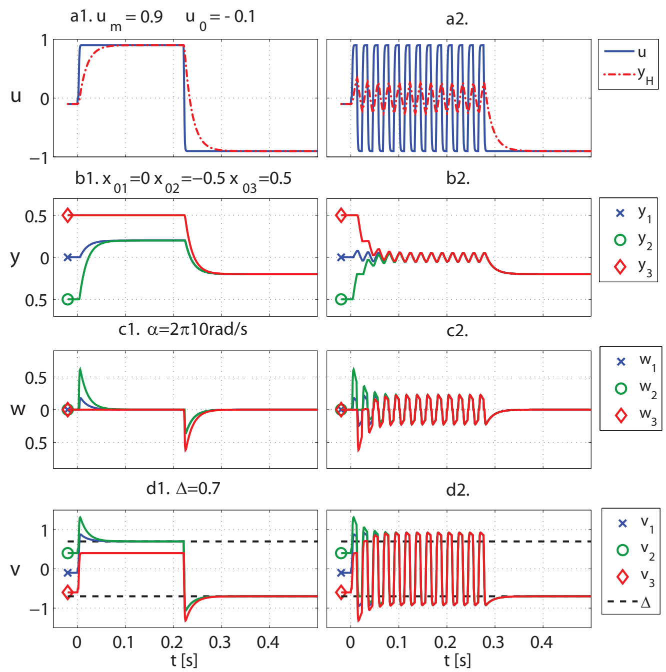

Fig. 6. Simulation of the nonlinear feedback model for three initial conditions with equal Δ and equal α. Begin and end conditions are u_0 and u_e. All intermediate signals y, w, v are shown. Subplot a. shows the response of the linear case y_H where $\Delta = 0$.

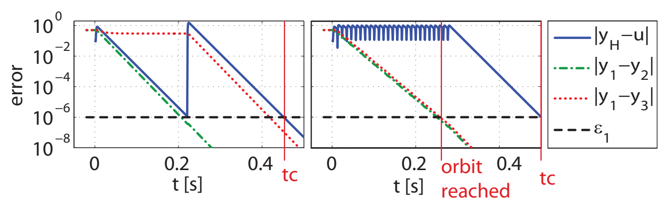

Fig. 7. Difference between the trajectories on a logarithmic scale. $|y_1 - y_2|$ vanishes for $u = u_m$, $|y_1 - y_3|$ for $u = -u_m$. (Compare with Fig. 6.). The error signal $|y_H - u|$ denotes the linearized case, which provides the initialization time. ϵ_1 denotes the allowed error.

Fig. 5 shows the convergence to an orbit starting from initial condition $x_0 = 0$ for three different sine wave frequencies. Due to the low-pass nature of the system, the area enclosed by the orbit displayed in the input output plot gets smaller with higher frequency. For quasi-static signals the boundary of area I of a single play operator is approached.

2) Stepwise Initialization: First the step response of a single section of a nonlinear feedback model with dead-zone is considered. The maximum magnitude of an applied step is $2u_m$. If, as in (4), an allowed deviation from the steady state output value $\bar{y}$ is defined as ϵ_1, then in worst case it takes the linear system t_H seconds to converge:

$$\begin{aligned} y_H(t) =& 2u_m(1 - e^{-\alpha t}) \\ |y_H - \bar{y}_H| =& 2u_m(e^{-\alpha t}) \leq \epsilon_1 \\ \Rightarrow t_H \geq& \frac{1}{\alpha} \ln\left(\frac{2u_m}{\epsilon_1}\right) \end{aligned} \tag{18}$$

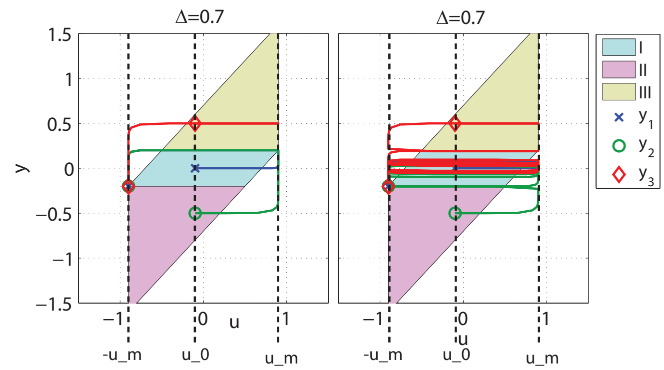

Fig. 8. Input-output plot for the simulation of Fig. 6. The trajectories start at $u_0, [x_{01}, x_{02}, x_{03}]$. They end at u_e, y_e. Each x_0 starts in a different region (I, II, III)

The step response of a system with $\Delta > 0$ can be rewritten as the step-response of H with magnitude $u - \Delta$ for $u - y > \Delta$ or $u + \Delta$ for $u - y < \Delta$. This magnitude is always less than $2u_m$ and, therefore, the convergence time for the linear system is the upper bound for systems with all possible dead-zone widths. For $|v| = |u - y| < \Delta$ the system's response remains constant. Note that in this model $x_0 = y_0$.

From the analysis of the multiplay a stepwise initialization profile was established: $u_0 \rightarrow u_m \rightarrow -u_m$. Since, the nonlinear feedback model approaches the multiplay model for quasi-static inputs the sequence will be successful if steady state is reached in between switching from one value to another. From the upper bound for a single step, the convergence time for this initialization approach is:

$$t_c = 2t_H = \frac{2}{\alpha} \ln\left(\frac{2u_m}{\epsilon_1}\right) \tag{19}$$

The left columns of Fig. 6, 7 and 8 shows the response of the model to the sequence for 3 different initial conditions. Since the first applied step is towards u_m, all trajectories starting from regions I and II are initialized. However, the status of trajectories starting from region III remains constant. In Fig. 7 the difference between the trajectories starting in the different regions are displayed along with the upper bound provided by the linear system.

At the moment that the linear system has converged for the step towards $-u_m$, all possible trajectories for systems with $u_m \geq \Delta$ are initialized to the point $(u, y) = (-u_m, -u_m + \Delta)$. Now for further quasi-static variation the resulting orbit is again the border of region I. Higher frequencies are dealt with next.

3) Square Wave Initialization: If the time between the initialization steps is less than t_H, initialization is not guaranteed within a single period. This is the case for a square wave input in the form $u_T = u_m \Phi(2\pi t/T + \theta) = u_m \text{sign}\{\sin(2\pi t/T + \theta)\}$, with $T/2 < t_H$.

However, by the use of multiple periods a unique orbit can still be reached. For the case $\Delta < u_m$ this is actually beneficial, since depending on the exact value of x_0, trajectories starting from II and III can be initialized at the same time

($u_m - y > \Delta$ and $-u_m - y < -\Delta$). For $\Delta \geq u_m$ multiple periods and a decreased T result in equal total duration as with the single period case.

This scenario is presented in the right columns of Fig. 6, 7, 8. The periodic orbit is reached sooner than in the stepwise case. However, if the source is switched to a constant value, in order to obtain a unique steady state output value, the system needs time to converge again (Fig. 7).

4) High Frequent Initialization: Despite the fact that the overall transfer from u to y has a low-pass behavior, there is no limit on $1/T$ concerning initialization. From the structure of the model, high frequencies in the input will directly enter the dead-zone $w = d_{2\Delta}(u - y)$. For a very short time (the time that $v \geq \Delta$) the system will respond. However, due to the high frequency the sum of all these moments is what initializes the system. A very high frequent excitation is thus capable of initializing the nonlinear feedback model with dead-zone.

V. DISCUSSION

A. Resulting Initialization Trajectories

Initialization of the Duhem model requires multiple periods. For two trajectories starting from different initial conditions the difference shrinks piecewise exponentially. However, the rate of convergence is slowed down by change of $\text{sign}(\dot{u})$. This supports the use of the maximum amplitude for initialization.

On the other hand, the multi-play model can be initialized with a single sequence containing both the maximum and minimum input. The same holds for the nonlinear feedback model with dead-zone. Multiple periods are only required if the time in between the steps is too short to converge within the required error bound. Multiple periods and a smaller period time is beneficial if $\Delta < u_m$, since trajectories starting in region II and III can converge at the same time.

All models agree on two points: Initialization trajectories should have maximum amplitude, and the initialization sequence should contain both the maximum and the minimum.

B. Model Artifacts

The properties of the initialization trajectories also reveal model artifacts. For the Duhem model this is the possibility to initialize the system using periodic signals with arbitrary small amplitude. For a large class of physical systems containing magnetic hysteresis this property does not correspond to the observed behavior, e.g. [17].

On the other hand, the state of nonlinear feedback models can be reset by signals with arbitrary high frequency. This will not be valid for e.g. spatially distributed ferromagnetic systems which deal with a limited skin depth for high frequent magnetic fields; It is not possible to initialize ferromagnetic objects with dm^3-volumes using a ultra-high frequent source with limited amplitude which results in skin depths $<< dm$.

VI. CONCLUSIONS

The notion of feed forward initialization for dynamical hysteretic systems is presented. The systems are step-convergent; the output converges to a constant for every constant input. Due to hysteresis the steady state value for a specific constant input depends on the initial conditions, instead of only the input as is the case with fading memory systems.

For different hysteresis models the properties of periodic input signals are determined such that they force the system into a unique orbit irrespective of the initial conditions. Once on this orbit the influence of initial conditions is erased.

For quasi-static inputs the rate-independent Duhem and multi-play hysteresis models are analyzed. Dynamic effects are included by the hysteretic nonlinear feedback model with dead-zone. Analysis using well established frameworks is possible since this model-class consists only of linear dynamics interconnected with static nonlinearities.

All models agree on the points that an initialization trajectory should have maximum amplitude and should contain at least both the maximum and the minimum input. For dynamical hysteretic systems, multiple periods are required if period time of the excitation to small compared to the model's time-constants.

REFERENCES

[1] B. Jayawardhana, H. Logemann, and E. P. Ryan, “Pid control of second-order systems with hysteresis,” *International Journal of Control*, vol. 81, no. 8, pp. 1331–1342, 2008.

[2] R. Iyer and X. Tan, “Control of hysteretic systems through inverse compensation,” *Control Systems Magazine, IEEE*, vol. 29, no. 1, pp. 83 –99, 2009.

[3] K. Kuhnen and P. Krejci, “Compensation of complex hysteresis and creep effects in piezoelectrically actuated systems;a new preisach modeling approach,” *IEEE Transactions on Automatic Control*, vol. 54, no. 3, pp. 537 –550, 2009.

[4] P. J. van Bree, C. M. M. van Lierop, and P. P. J. van den Bosch, “Electron microscopy experiments concerning hysteresis in the magnetic lens system,” in *Conference on Control Applications, CCA 2010*, 2010.

[5] J. H. Oh, B. Drincic, and D. S. Bernstein, “Nonlinear feedback models of hysteresis,” *Control Systems Magazine, IEEE*, vol. 29, no. 1, pp. 100 –119, 2009.

[6] J. H. Oh and D. S. Bernstein, “Semilinear duhem model for rate-independent and rate-dependent hysteresis,” *IEEE Transactions on Automatic Control*, vol. 50, no. 5, pp. 631–645, 2005.

[7] S. Boyd, L. El Ghaoui, E. Feron, and V. Balakrishnan, *Linear Matrix Inequalities in System and Control Theory*. Society for Industrial and Applied Mathematics (SIAM), 1994.

[8] I. Mayergoyz, *Mathematical models of hysteresis*. Springer, 1991.

[9] B. Coleman and M. Hodgdon, “On a class of constitutive relations for ferromagnetic hysteresis,” *Archive for Rational Mechanics and Analysis*, vol. 99, no. 4, pp. 375–396, 1987.

[10] R. Banning, W. L. De Koning, H. J. M. T. A. Adriaens, and R. K. Koops, “State-space analysis and identification for a class of hysteretic systems,” *Automatica*, vol. 37, no. 12, pp. 1883–1892, 2001.

[11] B. Drincic and D. S. Bernstein, “A multiplay model for rate-independent and rate-dependent hysteresis with nonlocal memory,” in *Decision and Control, Proceedings of the 48th IEEE Conference on*, 2009, pp. 8381 –8386.

[12] M. Al Janaideh, S. Rakheja, and C. Y. Su, “A generalized rate dependent play operator for characterizing asymmetric and symmetric hysteresis nonlinearities,” in *American Control Conference, 2008*, 2008, pp. 1911–1916.

[13] M. Krasnosel'skii, A. Pokrovskii, and M. Niezgodka, *Systems with hysteresis*. Berlin : Springer, 1989.

[14] A. Visintin, *Differential models of hysteresis*. Berlin : Springer, 1994.

[15] M. Brokate and J. Sprekels, *Hysteresis and Phase Transitions*. New York: Springer-Verlag, 1996.

[16] T. Pare, A. Hassibi, and J. How, “A kyp lemma and invariance principle for systems with multiple hysteresis non-linearities,” *International Journal of Control*, vol. 74, no. 11, pp. 1140–1157, 2001.

[17] P. J. van Bree, C. M. M. van Lierop, and P. P. J. van den Bosch, “Control-oriented hysteresis models for magnetic electron lenses,” *IEEE Transactions on Magnetics*, vol. 45, no. 11, pp. 5235–5238, 2009.